NUCL SCI TECH (2017) 28:69
DOI 10.1007/s41365-017-0222-y

Calculation of photon shielding properties for some neutron shielding materials

A. M. El-Khayatt[1,2]

Received: 15 June 2016 / Revised: 6 September 2016 / Accepted: 15 September 2016 / Published online: 31 March 2017
© Shanghai Institute of Applied Physics, Chinese Academy of Sciences, Chinese Nuclear Society, Science Press China and Springer Science+Business Media Singapore 2017

Abstract The objective of the present study is to calculate photon shielding parameters for seven polyethylene-based neutron shielding materials. The parameters include the effective atomic number (Z_{eff}), the effective electron density (N_{eff}) for photon interaction and photon energy absorption, and gamma-ray kerma coefficient (k_{γ}). The calculations of Z_{eff} are presented as a single-valued and are energy dependent. While Z_{eff} values were calculated via simplistic power-law method, the energy-dependent Z_{eff} for photon interaction ($Z_{PI\text{-}eff}$) and photon energy absorption ($Z_{PEA\text{-}eff}$) are obtained via the direct method for energy ranges of 1 keV–100 GeV and 1 keV–20 MeV, respectively. The k_{γ} coefficients are calculated by summing the contributions of the major partial photon interactions for energy range of 1 keV–100 MeV. In most cases, data are presented relative to pure polyethylene to allow direct comparison over a range of energy. The results show that combination of polyethylene with other elements such as lithium and aluminum leads to neutron shielding material with more ability to absorb neutron and γ-rays. Also, the kerma coefficient first increases with Z of the additive element at low photon energies and then converges with pure polyethylene at energies greater than 100 keV.

Keywords Neutron shielding materials · Effective atomic number · Kerma coefficient · γ-rays

✉ A. M. El-Khayatt
Ahmed_el_khayatt@yahoo.com; aelkhayatt@gmail.com

1 Physics Department, College of Science, Al Imam Mohammad Ibn Saud Islamic University (IMSIU), Riyadh, Saudi Arabia

2 Reactor Physics Department, NRC, Atomic Energy Authority, 13759 Cairo, Egypt

1 Introduction

Energetic radiations are of serious concern in nuclear powers and accelerator facilities, medical or industrial X-ray machines, and radioisotope production projects. So the radiation shielding is still an attractive topic for research, it aims to preserving both human safety and structural material which may be compromised from radiation exposure. Pure polyethylene (PE), with its high hydrogen concentration, is often used as a moderator to slow fast neutrons to thermal region. The combination of PE and other materials such as boron, lithium, or silicon makes it an effective neutron shielding material for different purposes. For example, borated PE is useful for neutron shielding in areas of low and intermediate neutron fluxes. Adding lithium to PE can be a shielding for both γ-rays and neutrons. Mixing the PE and silicon leads to neutron shielding with high resistance to fire. Finally, γ-ray shielding parameters are important for the neutron shielding materials that are used in the presence of γ-rays or may be exposed to γ-rays from the (n, γ) reactions.

Effective atomic number (Z_{eff}) and effective electron density (N_{eff}) are useful parameters for describing radiation interaction with composite matter, in terms of equivalent elements. Many authors reported on γ-ray attenuation parameters for concretes [1–3], glasses [4–7], lunar soil samples [8], building materials [9], alloys [10], low-Z materials [11, 12], and other materials [13, 14]. However, plenty of them are usually restricted to a candidate γ-ray shielding material or to low-Z materials, which are more important in medical physics. Moreover, the γ-ray shielding properties seem to be limited to photon attenuation properties only, such as linear attenuation coefficient (μ), mass attenuation coefficients (μ/ρ), and effective atomic numbers. In any case, kerma, K, subject had scarcely treated [15].

The kerma, an acronym for "kinetic energy released in materials," has replaced the traditional exposure as the shielding design parameter [16]. In fact, gamma heating is the local energy deposition from γ-ray interactions. Often, this can be done by estimating the kerma. To relate the radiation passing through a unit volume of a material of interest (fluence, Φ) to the energy release, K, in the material, the phrase "fluence-to-kerma factors" has been introduced by International Commission on Radiological Units and Measurements, ICRU [17] and widely used [18–20]. However, instead of using kerma factor, the kerma coefficient (k_γ, kerma per fluence) will be used throughout this paper, as the word coefficient implies a physical dimension, whereas the word factor does not [21]. Kerma coefficient is of interest for biomedical applications, because it is used to convert photon fluence-to-kerma (absorbed dose). Also, kerma coefficient, which is the key response function for nuclear heating, is important in many nuclear applications, particularly for fission and fusion power reactors [18, 20, 22].

In this work, we aimed at calculating photon shielding energy-dependent parameters for seven polyethylene-based neutron shielding materials. The parameters include Z_{eff} and N_{eff} for both photon interaction and photon energy absorption for the energy regions of 1 keV–100 GeV and 1 keV–20 MeV, respectively. The k_γ was calculated for the energy region of 1 keV–100 MeV. For many cases, the results are presented relative to pure PE to allow direct comparison over a range of energy. Finally, we are also discussing the single-valued Z_{eff} and N_{eff} generated by the simple power-law method, whereby the elemental constituents of a material are summed (weighted according to their atomic percentage or to their relative electron fraction) and raised to a power.

2 Computational method and theoretical basis

2.1 The single-valued effective atomic number

A simple way to evaluate Z_{eff} is the use of a simple power law:

$$Z_{eff} = \left(\sum_i a_i^e Z_i^m\right)^{1/m}, \tag{1}$$

where Z_i is atomic number of the ith element, and a_i^{e} its fractional electronic content. In fact, the researchers consider different values for the exponent m, such as m was 2.94, 3.1, 3.4, and 3.5 by Mayneord [23], Hine [24], Tsaï and Cho [25], and Sellakumar et al. [26]. In addition, the corresponding electron density N_{eff} is given by

$$N_{\text{eff}} = N_{\text{A}}\left(\sum_i a_i^{\text{e}}(Z_iA_i)\right), \tag{2}$$

where A_i is the atomic mass, and N_{A} is the Avogadro's constant.

Also, the Z_{eff} can be given by atomic percentage of each element, α_i^{at}, which is defined by the mass percentage w_i and A_i:

$$\alpha_i^{\text{at}} = \frac{(w_i/A_i)}{\sum_i (w_i/A_i)}. \tag{3}$$

The literature review showed two more definitions: Eq. (4) by Puumalainen et al. [27] and Eq. (5) by Manninen et al. [28].

$$Z_{\text{eff}} = \left(\frac{\sum_i \alpha_i^{\text{at}} Z_i^3}{\sum_i \alpha_i^{\text{at}} Z_i}\right)^{1/2}, \tag{4}$$

$$Z_{eff} = \sum_i \alpha_i^{at} Z_i. \tag{5}$$

It can easily be shown that a_i^{e} and α_i^{at} are very nearly equal.

Finally, Murty suggested a more simple expression for calculating the Z_{eff} [29],

$$Z_{\text{eff}} = \left(\sum_i w_i Z_i^{3.1}\right)^{1/3.1} \tag{6}$$

On the other hand, the average electron density is given by

$$\langle N\rangle = N_{\text{A}}\frac{\langle A\rangle}{\langle Z\rangle}, \tag{7}$$

where $<A>$ and $<Z>$ is the mean atomic mass and the mean atomic number, respectively:

$$\langle A\rangle = \sum_i f_i A_i, \tag{8}$$

$$\langle Z\rangle = \sum_i f_i Z_i, \tag{9}$$

where A is the atomic mass, Z is the atomic number, and f_i is the molar fraction of the ith element (normalized so that $\sum f_i = 1$).

This simple approach, however, is approximately valid at low energies where photoelectric absorption is dominating and is overly simplistic for many applications.

2.2 Calculation of energy-dependent Z_{eff} and N_{eff}

Energy-dependent Z_{eff} has been described elsewhere [30] in a more rigorous fashion; here, only the final equations are given.

$$Z_{\mathrm{PI-eff}} = \frac{\sum_i f_i A_i \left(\frac{\mu}{\rho}\right)_i}{\sum_i f_i \frac{A_i}{Z_i} \left(\frac{\mu}{\rho}\right)_i}, \tag{10}$$

where (μ_{en}/ρ) is the mass attenuation coefficient. NXcom program has been used to calculate the mass attenuation coefficients for the energy range of 1 keV–100 GeV [31]. The effective electron density, $N_{\text{PI-eff}}$, is given by (in electron per gram):

$$N_{\mathrm{PI-eff}} = N_{\mathrm{A}} \frac{N_{\mathrm{PI-eff}}}{\langle A \rangle}. \tag{11}$$

The effective atomic number ($Z_{\text{PEA-eff}}$) and the effective electron density ($N_{\text{PEA-eff}}$) for photon energy absorption can be obtained from Eqs. (10) and (11), respectively. Mass energy-absorption coefficients are calculated for the studied object at photon energies using the photon data from Hubbell and Seltzer [32].

2.3 Computation of photon kerma coefficients

The kerma, K, is the quotient of $\mathrm{d}E_{\mathrm{tr}}$ by $\mathrm{d}m$, where $\mathrm{d}E_{\mathrm{tr}}$ is the mean sum of the initial energies of all charged particles liberated by indirectly ionizing radiations such as neutrons and photons in a mass $\mathrm{d}m$ of a material [33], thus

$$K = \mathrm{d}E_{\mathrm{tr}}/\mathrm{d}m, \tag{12}$$

For a fluence, Φ, of uncharged particles of energy E, K in a specified material is given by

$$K = \Phi E(\mu_{\mathrm{tr}}/\rho) = \Psi(\mu_{\mathrm{tr}}/\rho), \tag{13}$$

where (μ_{tr}/ρ) is the mass energy-transfer coefficient of the material for these particles, and Ψ is the energy fluence. The kerma per fluence, K/Φ, is termed the kerma coefficient, k, for uncharged particles of energy E in a specified material, thus

$$k = K/\Phi = E(\mu_{\mathrm{tr}}/\rho). \tag{14}$$

For low-Z materials (e.g., air, water, and soft tissue), only a small part is expended in bremsstrahlung (collisions with atomic nuclei). Therefore, mass energy-transfer coefficient (μ_{tr}/ρ) and mass energy mass energy-absorption coefficient (μ_{en}/ρ) are almost equal. Thereby, photon kerma coefficients (in Gy·cm^2/photon) of such materials can be obtained by Eq. (15):

$$k_\gamma = k_{\mathrm{D}} E_\gamma \sum_i w_i [\mu_{\mathrm{en}}(E_\gamma)/\rho]_i, \tag{15}$$

where $k_D = 1.602 \times 10^{-10}$ Gy g/MeV is the energy conversion coefficient.

On the other hand, when the bremsstrahlung production is not negligible, the major contributing reactions for gamma kerma coefficients (in Gy cm^2/photon) in the energy range of fusion systems are the photoelectric (Pe), Compton scattering (C), pair production reactions (pp), and coherent (no energy loss) [18]:

$$k_\gamma = k_{\mathrm{D}} \sum_i w_i \left[\sigma^i_{\mathrm{Pe}} E_\gamma + \sigma^i_{\mathrm{pp}}(E_\gamma - 1.022) + \sigma^i_{\mathrm{C}}\left(E_\gamma - E^i_\gamma\right)\right], \tag{16}$$

where σ^i_{pe}, σ^i_{pp}, and σ^i_C are photoelectric, pair production, and Compton absorption cross sections for element i, respectively. It is important to recognize that above 5 MeV one in principle should include photonuclear absorption cross section $\sigma_{ph.n}$. However, this process is not readily amenable to systematic calculation and tabulation. Hence, $\sigma_{ph.n}$ is ignored in current compilations, even though at its giant resonance peak between 5 and 40 MeV it can contribute between 2% (high-Z elements) and 6% (low-Z elements) to the total cross section σ_{tot} [34].

Implicit in the use of Eq. (16) is the assumption that all the gamma photon energy in the photoelectric process is deposited locally and in pair production, 1.022 MeV (energy of electron–positron masses) of the photon energy is not available for local deposition. In the Compton scattering reaction, the photon only deposits a fraction of its energy locally because the scattered photon carries the rest away.

3 Results and discussion

The chemical composition of neutron shielding materials studied in the present work is given in Table 1 [35], for combinations of PE and other materials such as boron, lithium, or silicon. The single-valued calculated energy-dependent Z_{eff} and N_{eff} for all samples are listed in Table 2.

Examples of such calculations are graphed in Fig. 1. The single-valued effective atomic numbers are only a rough approximation at low energies and should be treated with some caution. At medium photon energies (about 0.5–3.5 MeV) where Compton scattering process is the most probable, one can notice that the Z_{eff} and N_{eff} are approximately equal to their mean values $<Z>$ and $<N>$, respectively. Therefore, the mean values can represent Z_{eff} and N_{eff} at medium photon energies only.

3.1 The effective atomic number

The calculated values of energy-dependent $Z_{\text{PI-eff}}$, $N_{\text{PI-eff}}$, $Z_{\text{PEA-eff}}$, and $N_{\text{PEA-eff}}$ for PE and six neutron shielding materials, and the ratios of $(Z_{\text{PI-eff}})^{\text{m}}_{\text{PE}}$, $(N_{\text{PI-eff}})^{\text{m}}_{\text{PE}}$, $(Z_{\text{PEA-eff}})^{\text{m}}_{\text{PE}}$, and $(N_{\text{PEA-eff}})^{\text{m}}_{\text{PE}}$ are shown in Fig. 2, as a function of photon energy. The energy dependence of $Z_{\text{PI-eff}}$ (for total photon interaction) for all the neutron shielding materials

Table 1 Elemental composition (wt%) of neutron shielding materials

Sample no.	H	Li	B	C	O	Na	Mg	Al	Si	S	Cl	Ca	Ti	Mn	Fe	Zn	Sr
238	2.76	–	25.35	20.08	24.15	–	–	–	26.93	–	–	0.04	0.02	–	0.41	0.26	–
207HD	6.01	–	0.86	18.02	48.42	0.17	0.02	24.9	0.04	0.01	–	1.36	–	–	0.01	–	0.06
210	8.54	–	30	59.25	0.76	–	–	0.04	1.01	–	–	–	–	0.02	0.38	–	–
2015	8.6	7.5	0	57.76	26.13	0.001	–	–	–	–	0.004	0.001	–	–	–	–	–
261	8.94	–	10	36.65	44.41	–	–	–	–	–	–	–	–	–	–	–	–
201	11.6	–	5	61.2	22.2	–	–	–	–	–	–	–	–	–	–	–	–
213	14.4	–	–	85.6	–	–	–	–	–	–	–	–	–	–	–	–	–

Table 2 The mean atomic mass, mean atomic number, average electron density and single-valued Z_{eff} and N_{eff} of neutron shielding materials

Sample no.	<*A*>	<*N*>	Z_{eff}						N_{eff}* ($\times 10^{23}$ e g^{-1})	<*N*> ($\times 10^{23}$ e g^{-1})
			Reference [29]	Reference [20]	Reference [24]	Reference [25]	Reference [26]	Reference [28]		
238	10.83	5.45	10.37	10.15	10.30	10.52	10.67	9.25	3.12	3.03
207HD	8.66	4.54	10.01	9.66	9.77	9.93	10.06	9.00	3.32	3.16
213	7.23	3.87	8.82	8.70	8.62	6.95	6.96	6.66	3.41	3.22
261	6.40	3.46	6.85	6.64	6.67	6.70	6.75	6.39	3.48	3.25
215	6.23	3.34	6.41	6.22	6.26	6.29	6.34	5.97	3.46	3.23
210	6.15	3.26	6.53	6.21	6.34	6.59	6.73	5.62	3.42	3.19
201	5.42	3.01	6.33	6.09	6.12	6.15	6.20	5.82	3.61	3.34

* Reference [26]

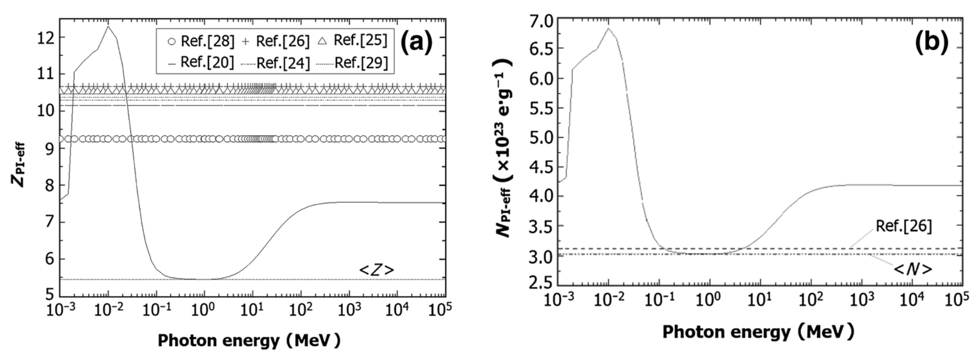

Fig. 1 The single-valued calculated energy-dependent $Z_{PI\text{-}eff}$ (**a**) and $N_{PI\text{-}eff}$ (**b**) for Sample 238 and the mean atomic number

has almost the same behavior. One can see that the curves of Z_{eff} are arranged in descending order according to their mean atomic number <*Z*>. Figure 2a shows three energy regions, where Z_{eff} is almost constant "plateau" for a given material, while the transition regions are characterized by a rapid variation of Z_{eff}. This energy behavior of Z_{eff} reflects relative importance of the three γ-ray processes: photoelectric, Compton, and pair production. The plateau region is formed when only one photon interaction is dominant, whereas the transition one includes more than one interaction which makes significant contributions to the total interaction. Therefore, we have three plateaus corresponding to the dominance regions of the three γ-ray interactions, photoelectric absorption ($E < 0.01$ MeV), Compton scattering ($0.1 < E < 6$ MeV), and pair production ($E > 200$ MeV). In addition, two transition regions ($0.01 < E < 0.1$ MeV) and ($6 < E < 200$ MeV) are observed.

At a given photon energy, the interaction is proportional to Z^n where n is about 4 for the photoelectric absorption, 1 for the Compton scattering, and 2 for pair production. The Z^4 dependence of the photoelectric absorption cross section

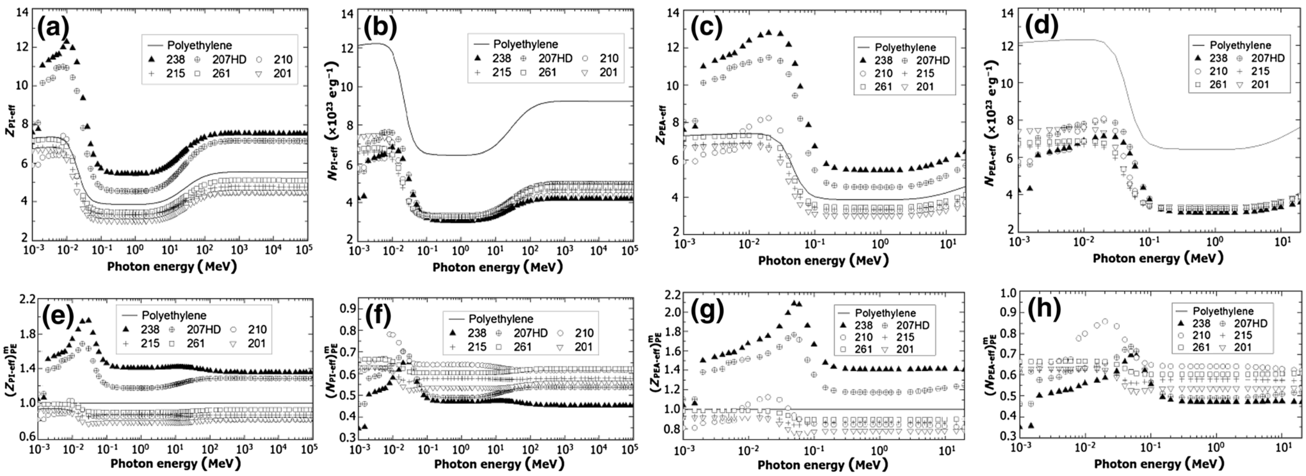

Fig. 2 $Z_{\text{PI-eff}}$ (**a**), $N_{\text{PI-eff}}$ (**b**), $Z_{\text{PEA-eff}}$ (**c**), and $N_{\text{PEA-eff}}$ (**d**) of the neutron shielding materials and their ratios to as function of photon energy

leads to heavy weight to the element with the highest atomic number, and the maximum value of Z_{eff} is found in the region of photoelectric plateau. At intermediate energies, Compton scattering is the main interaction process, and Z_{eff} is close to the mean atomic number of the material, as the Compton scattering cross section of an element is proportional to Z. The minimum value of Z_{eff} is recorded in this intermediate plateau. Above 200 MeV, the pair production plateau is observed, where Z_{eff} is almost constant and its mean value is smaller than that obtained for photoelectric plateau. This is due to the fact that the pair production cross section is proportional to Z^2, giving less weight to the higher-Z elements than the photoelectric absorption cross section. The same arguments also hold for $Z_{\text{PEA-eff}}$ as shown in Fig. 2c.

To compare the Z_{eff} values of a given PE-based shielding material with that of polyethylene, Fig. 2e–h presents the ratios of Z_{eff} of the materials for photon interaction and photon energy absorption to those of PE as a function of photon energy. Figure 2e, g shows that the materials containing higher-Z elements, such as samples 238 and 207HD, have Z_{eff} values systematically greater than that of PE over the full energy range studied. Such neutron shielding materials have a competitive advantage in attenuating gamma rays.

3.2 The effective electron density

Figure 2b, d shows the energy dependence of N_{eff} for total photon interaction and photon energy absorption, respectively. Figure 2f, h presents the N_{eff} ratios with respect to PE. The behavior is similar to that of Z_{eff}, because the two parameters are closely related through Eq. (7). However, in contrast to Z_{eff}, the obtained curves for N_{eff} are not arranged by their average electron density $\langle N \rangle$ (Table 1). Thus, we can conclude that the average electron density of the material does not give us any correct indication of real effective electron-density value. Finally, it is obvious that the different single-valued effective atomic numbers, which are estimated using simple power law, are approximately valid at low energies where photoelectric absorption is dominating as shown in Fig. 1.

3.3 Kerma coefficients

The energy dependence of γ-ray kerma coefficient, which depends on the photon interaction cross sections, is shown in Fig. 3. Surprisingly, there is no plateau, and only rapid variation of k_γ with energy is seen. The kerma coefficient curves of the studied materials have dips in the energy range of around 0.3–0.09 MeV, and the dip position shifts to higher energy with increasing concentration of high-Z elements. We have also seen the K- and L-absorption edges in graphs of 210, 207HD, and 238 samples due to the presence of high-Z elements such as Zn and Sr (Table 3). Figure 3 also shows that the k_γ curves tend to

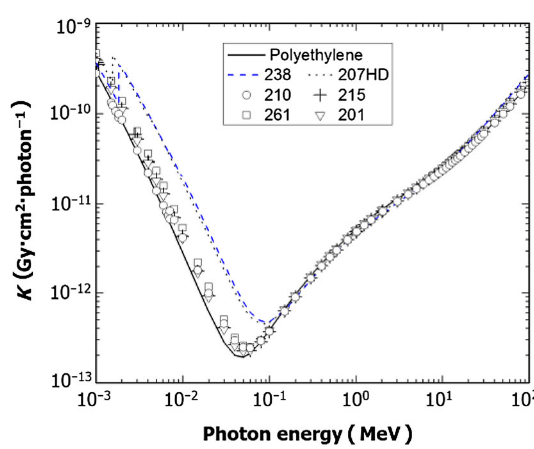

Fig. 3 Gamma-ray kerma coefficients for neutron shielding materials and polyethylene as a function of photon energy

Table 3 Photon energies (in keV) of absorption edges above 1 keV

Elements	Z	L3	L2	L1	K
Na	11	–	–	–	1.07
Mg	12	–	–	–	1.31
Al	13	–	–	–	1.56
Si	14	–	–	–	1.84
S	16	–	–	–	2.47
Ca	20	–	–	–	4.04
Ti	22	–	–	–	4.97
Mn	25	–	–	–	6.54
Fe	26	–	–	–	7.11
Zn	30	1.02	1.04	1.19	9.66
Sr	38	1.94	2.01	2.22	16.10

converge after departure of the photoelectric absorption dominance region ($E > 0.1$ MeV), where the other photon interaction processes give less weight to the higher-Z additive elements than that given by photoelectric process.

4 Conclusions

1. Combination of polyethylene with other elements such as lithium and aluminum leads to neutron shielding material with more ability to absorb neutron capture γ-rays; therefore, these materials are good shielding for neutron and gamma ray.
2. Variations of Z_{eff} and N_{eff} with photon energy showed three basic energy plateaus and two transition regions which are characterized by a rapid variation of Z_{eff} and N_{eff}. Both plateaus and transition regions were attributed to the dominance of one and more photon interaction processes, respectively.
3. The three energy plateaus are approximately $E < 0.01$ MeV, $0.1\ \text{MeV} < E < 6$ MeV, and $E > 200$ MeV.
4. The single-valued effective atomic numbers are calculated by different six expressions, and the results are approximately valid at low energies Therefore, it should be treated with some caution.
5. The energy dependence of γ-ray kerma coefficients showed rapid variations with energy, and they have dips in the energy range of around 0.3–0.9 MeV.
6. All curves of γ-ray kerma coefficients converge at energies greater than 0.1 MeV.

References

1. I. Akkurt, A.M. El-Khayatt, Effective atomic number and electron density of marble concrete. J. Radioanal. Nucl. Chem. **259**(1), 633–638 (2013). doi:10.1016/j.anucene.2013.04.021
2. E. Yılmaz, H. Baltas, E. Kırısa et al., Gamma-ray and neutron shielding properties of some concrete materials. Ann. Nucl. Energy **38**(10), 128–132 (2011). doi:10.1016/j.anucene.2011.06.011
3. M. Kurudirek, Radiation shielding and effective atomic number studies in different types of shielding concretes, lead base and non-lead base glass systems for total electron interaction: a comparative study. Nucl. Eng. Des. **280**, 440 (2014). doi:10.1016/j.nucengdes.2014.09.020
4. N. Chanthima, J. Kaewkhao, P. Limsuwan, Study of photon interactions and shielding properties of silicate glasses containing Bi_2O_3, BaO and PbO in the energy region of 1 keV to 100 GeV. Ann. Nucl. Energy **41**, 119 (2012). doi:10.1016/j.anucene.2011.10.021
5. S. Ruengsri, S. Insiripong, N. Sangwaranatee et al., Development of barium borosilicate glasses for radiation shielding materials using rice husk ash as a silica source. Prog. Nucl. Energy **83**, 99 (2015). doi:10.1016/j.pnucene.2015.03.006
6. A.M. El-Khayatt, A.M. Ali, V.P. Singh, Photon attenuation coefficients of heavy-metal oxide glasses by MCNP, XCOM program and experimental data: a comparison study. Nucl. Instrum. Methods Phys. Res. A **735**, 207–212 (2014). doi:10.1016/j.nima.2013.09.027
7. N. Chanthima, J. Kaewkhao, Investigation on radiation shielding parameters of bismuth borosilicate glass from 1 keV to 100 GeV. Ann. Nucl. Energy **55**, 23 (2013). doi:10.1016/j.anucene.2012.12.011
8. A.M. El-Khayatt, M.A. Al-Rajhi, Analysis of some lunar soil and rocks samples in terms of photon interaction and photon energy absorption. Adv. Space Res. **55**(7), 1816–1822 (2015). doi:10.1016/j.asr.2015.01.020
9. V.P. Singh, N.M. Badiger, A.M. El-Khayatt, Study on gamma-ray exposure buildup factors and fast neutron shielding properties of some building materials. Radiat. Eff. Defects Solids **169**(6), 547–559 (2014). doi:10.1080/10420150.2014.905942
10. P. Limkitjaroenporn, J. Kaewkhao, S. Asavavisithchai, Determination of mass attenuation coefficients and effective atomic numbers for Inconel 738 alloy for different energies obtained from Compton scattering. Ann. Nucl. Energy **53**, 64 (2013). doi:10.1016/j.anucene.2012.08.020
11. A.M. El-Khayatt, A.M. Ali, V.P. Singh et al., Determination of mass attenuation coefficient of low-Z dosimetric materials. Radiat. Eff. Defects Solids **169**(12), 1038–1044 (2014). doi:10.1080/10420150.2014.988626
12. M. Kurudirek, Effective atomic numbers and electron densities of some human tissues and dosimetric materials for mean energies of various radiation sources relevant to radiotherapy and medical applications. Radiat. Phys. Chem. **1021**, 39 (2014). doi:10.1016/j.radphyschem.2014.04.033
13. M. Kurudirek, Effective atomic number, energy loss and radiation damage studies in some materials commonly used in nuclear applications for heavy charged particles such as H, C, Mg, Fe, Te, Pb and U. Radiat. Phys. Chem. **122**, 15 (2016). doi:10.1016/j.radphyschem.2016.01.012
14. P. Limkitjaroenporn, J. Kaewkhao, Gamma-rays attenuation of zircons from Cambodia and South Africa at different energies: a new technique for identifying the origin of gemstone. Radiat. Phys. Chem. **103**, 67 (2014). doi:10.1016/j.radphyschem.2014.05.035
15. A.M. El-Khayatt, H.R. Vega-Carrillo, Photon and neutron kerma coefficients for polymer gel dosimeters. Nucl. Instrum. Methods Phys. Res. A **792**, 6–10 (2015). doi:10.1016/j.nima.2015.04.033
16. J.E. Turner, *Atoms, Radiation, and Radiation Protection*, 3rd edn. (WILEY GmbH & Co. KGaA, Weinheim, 2007)
17. ICRU Report 84, *Radiation Quantities and Units* (International Commission on Radiation Units and Measurements, Bethesda, MD, 1962)

18. L. Zhang, M.A. Abdou, Kerma factor evaluation and its application in nuclear heating experiment analysis. Fusion Eng. Des. **36**, 479–503 (1997). doi:10.1016/S0920-3796(96)00704-1
19. R.S. Caswell, J.J. Coyne, M.L. Randolph, Int. J. Appl. Radiat. Isot. **33**(11), 1227–1262 (1982). doi:10.1016/0020-708X(82)90246-0
20. M.A. Abdou, C.W. Maynard, Calculational methods for nuclear heating-part I: theoretical and computational algorithms. Nucl. Sci. Eng. **56**(4), 360–380 (1975)
21. ICRU Report 85, Fundamental quantities and units for ionizing radiation (revised). J. ICRU **11**(1), 22 (2011). doi:10.1093/jicru/ndr009
22. H.C. Claiborne, M. Solomito, J.J. Ritts, Heat generation by neutrons in some moderating and shielding materials. Nucl. Eng. Des. **15**, 232–236 (1971). doi:10.1016/0029-5493(71)90065-3
23. M. Faiz Khan, *The Physics of Radiation Therapy* (Williams and Wilkins Publishers, Baltimore, MD, 1994)
24. G.E. Hine, Secondary electron emission and effective atomic numbers. Nucleonics **10**(1), 9–15 (1952). CODEN: NUCLAM; ISSN: 0096-6207
25. C.M. Tsaï, Z.H. Cho, Physics of contrast mechanism and averaging effect of linear attenuation coefficients in a computerized transverse axial tomography (CTAT) transmission scanner. Phys. Med. Biol. **21**(4), 544–559 (1976). doi:10.1088/0031-9155/21/4/006
26. P. Sellakumar, E.J.J. Samuel, S.S. Supe, Water equivalence of polymer gel dosimeters. Radiat. Phys. Chem. **76**(7), 1108–1115 (2007). doi:10.1016/j.radphyschem.2007.03.003
27. P. Puumalainen, H. Olkkonen, P. Sikanen, Assessment of fat content of liver by a photon scattering technique. Int. J. Appl. Radiat. Isot. **28**(9), 785–787 (1977). doi:10.1016/0020-708X(77)90110-7
28. S. Manninen, T. Pitkanen, S. Koikkalainen, T. Paakkari, Determination of the effective atomic number using elastic and inelastic scattering of γ-rays. Int. J. Appl. Radiat. Isot. **35**(10), 965–968 (1984). doi:10.1016/0020-708X(84)90212-6
29. R.C. Murty, Effective atomic numbers of heterogeneous materials. Nature **207**, 398–399 (1965). doi:10.1038/207398a0
30. S.R. Manohara, S.M. Hanagodimath, K.S. Thind et al., The effective atomic number revisited in the light of modern photon-interaction cross-section databases. Appl. Radiat. Isot. **68**(4–5), 784–787 (2010). doi:10.1016/j.apradiso.2009.09.047
31. A.M. El-Khayatt, NXcom—a program for calculating attenuation coefficients of fast neutrons and gamma-rays. Ann. Nucl. Energy **38**(1), 128–132 (2011). doi:10.1016/j.anucene.2010.08.003
32. J.H. Hubbell, S.M. Seltzer, *Tables of X-ray mass attenuation coefficients and mass energy-absorption coefficients 1 keV to 20 MeV for elements Z = 1 to 92 and 48 additional substances of dosimetric interest NISTIR 5632* (National Institute of Standards and Technology, Gaithersburg, 1995)
33. F.H. Attix, *Introduction to Radiological Physics and Radiation Dosimetry* (Wiley, New York, 1986)
34. J.H. Hubbell, Review of photon interaction cross section data in the medical and biological context. Phys. Med. Biol. **44**, R1 (1999). doi:10.1088/0031-9155/44/1/001
35. Bladewerx Company, http://www.shieldwerx.com